Supporting Information

Design and Synthesis of Bubble-Nanorod-Structured Fe_2O_3–Carbon Nanofibers as Advanced Anode Material for Li-Ion Batteries

*Jung Sang Cho, Young Jun Hong, and Yun Chan Kang**

* Corresponding author: yckang@korea.ac.kr

This file includes:

- XPS spectra of the (a) - (c) nanofibers post-treated at 500 °C under H_2/Ar atmosphere and (d) - (f) subsequent heat treated nanofibers at 300 °C under air atmosphere.
- XRD patterns of (a) nanofibers after stabilization process at 220 ^oC in air atmosphere and (b) subsequent treated nanofibers at 500 °C under H_2/Ar mixed gas atmosphere.
- (a) TEM and (b) HR-TEM images of Fe_3C spheres in the structure of FeO_x–carbon composite nanofibers after heat-treatment at 500 °C under H_2/Ar gas atmosphere.
- N_2 gas adsorption and desorption isotherms and pore size distributions: (a) and (b) hollow Fe_2O_3 nanofiber and (c) and (d) bubble-nanorod-structured Fe_2O_3-C nanofiber.
- Morphologies of the (a)-(c) bubble–nanorod-structured Fe_2O_3–C composite nanofibers and (d)-(f) hollow bare Fe_2O_3 nanofibers obtained after 300 cycles.
- SEM image of electrospun nanofibers.
- TG analysis of nanofibers post-treated at 500 °C under H_2/Ar atmosphere.
- FE-SEM image of bubble-rod-structured Fe_2O_3-C composite nanofiber.
- Digital photos and SEM images of the nanofibers otained at a different post-treatment temperatures under air.: (a),(b) 300 ^oC, (c),(d) 400 ^oC, (e),(f) 500 ^oC.

- Electrochemical properties of the bubble-nanorod-structured Fe_2O_3-C composite nanofibers using the anode prepared by mixing the active material, carbon black, and sodium carboxymethyl cellulose (CMC) in a weight ratio of 8:1:1: (a) cycling performance and (b) rate performance.

- Electrochemical properties of FeO_x–carbon composite nanofibers after thermal-treatment at 500 ^{o}C under H_2/Ar gas atmosphere: (a) cycling performance and (b) charge-discharge curves.

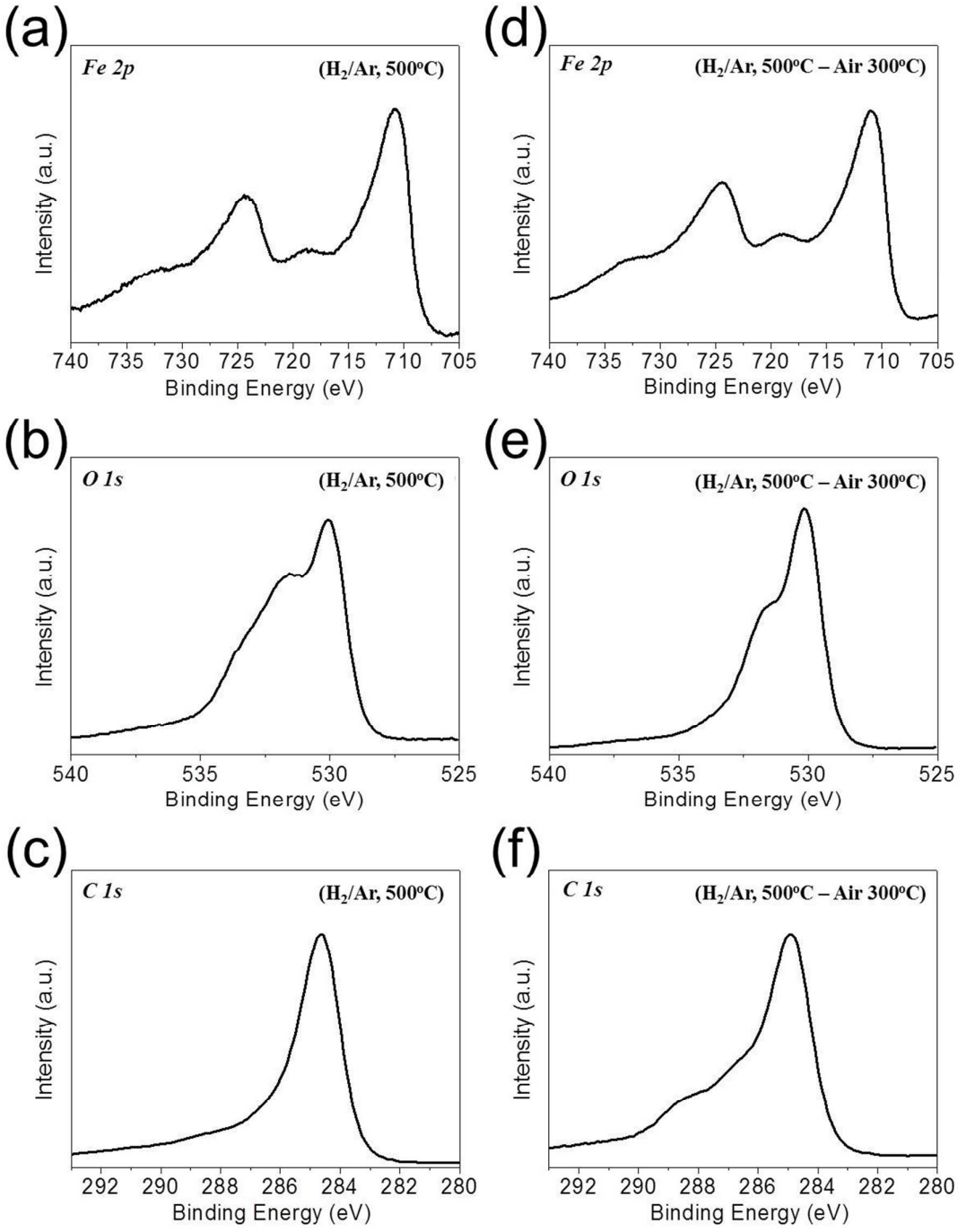

Figure S1. XPS spectra of the (a) - (c) nanofibers post-treated at 500 °C under H_2/Ar atmosphere and (d) - (f) subsequent heat treated nanofibers at 300 °C under air atmosphere.

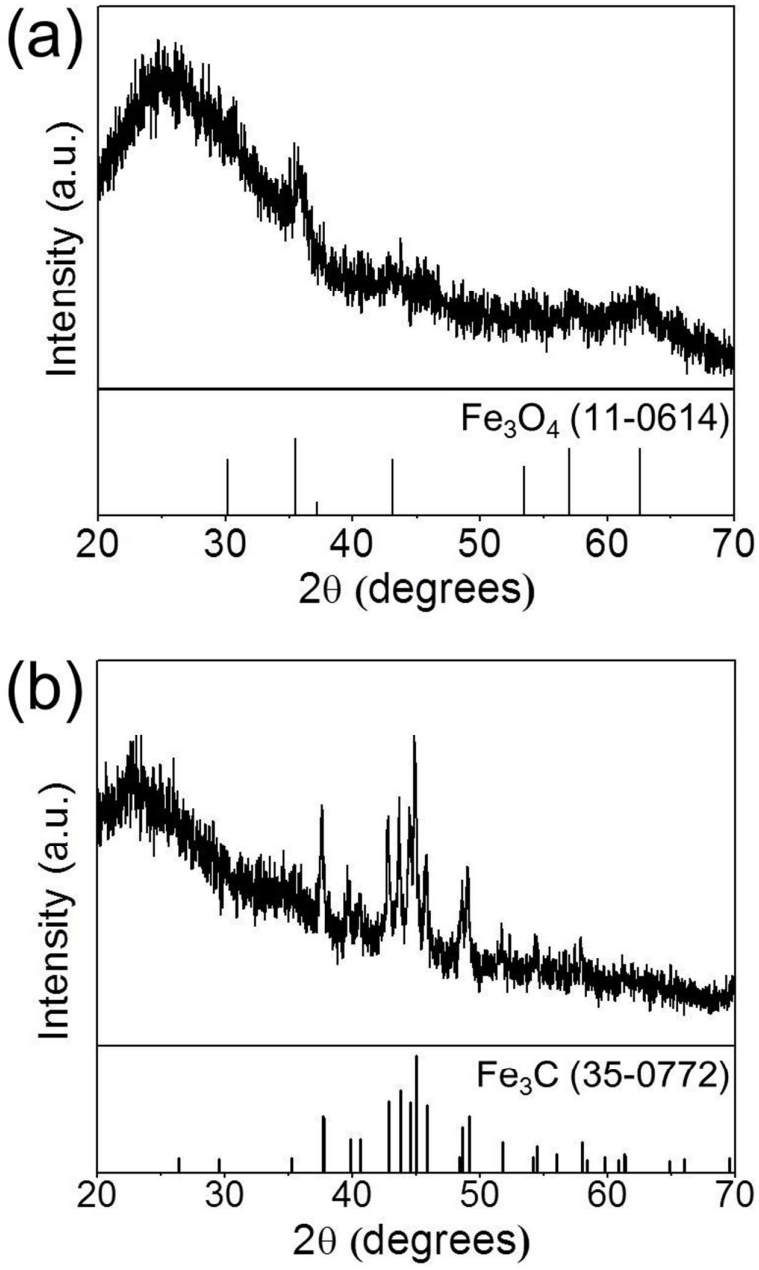

Figure S2. XRD patterns of (a) nanofibers after stabilization process at 220 ^{o}C in air atmosphere and (b) subsequent treated nanofibers at 500 °C under H_2/Ar mixed gas atmosphere.

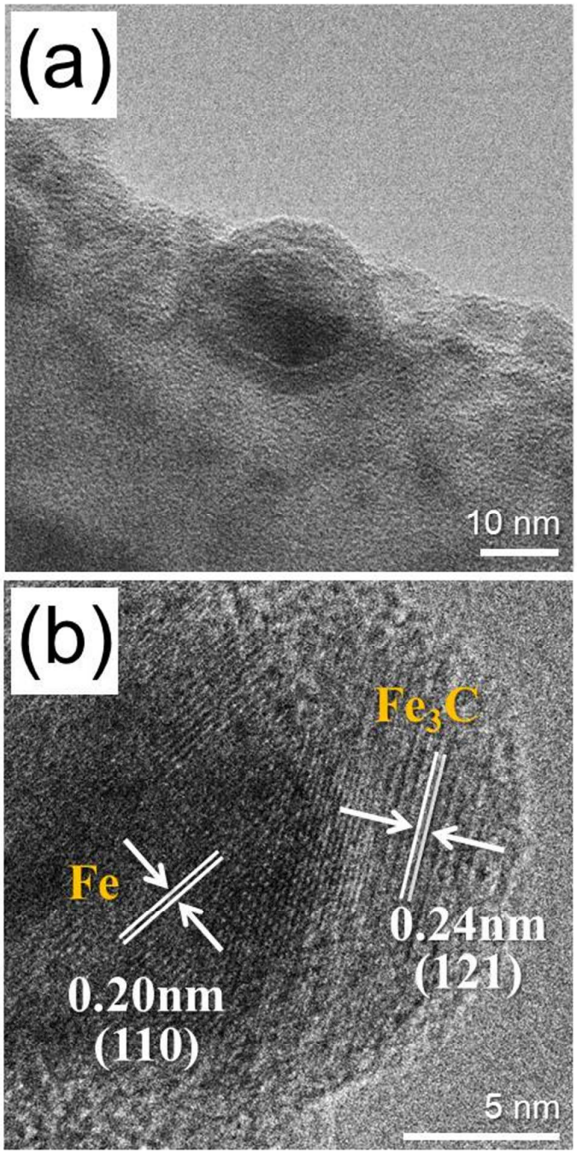

Figure S3. (a) TEM and (b) HR-TEM images of Fe_3C spheres in the structure of FeO_x–carbon composite nanofibers after heat-treatment at 500 °C under H_2/Ar gas atmosphere.

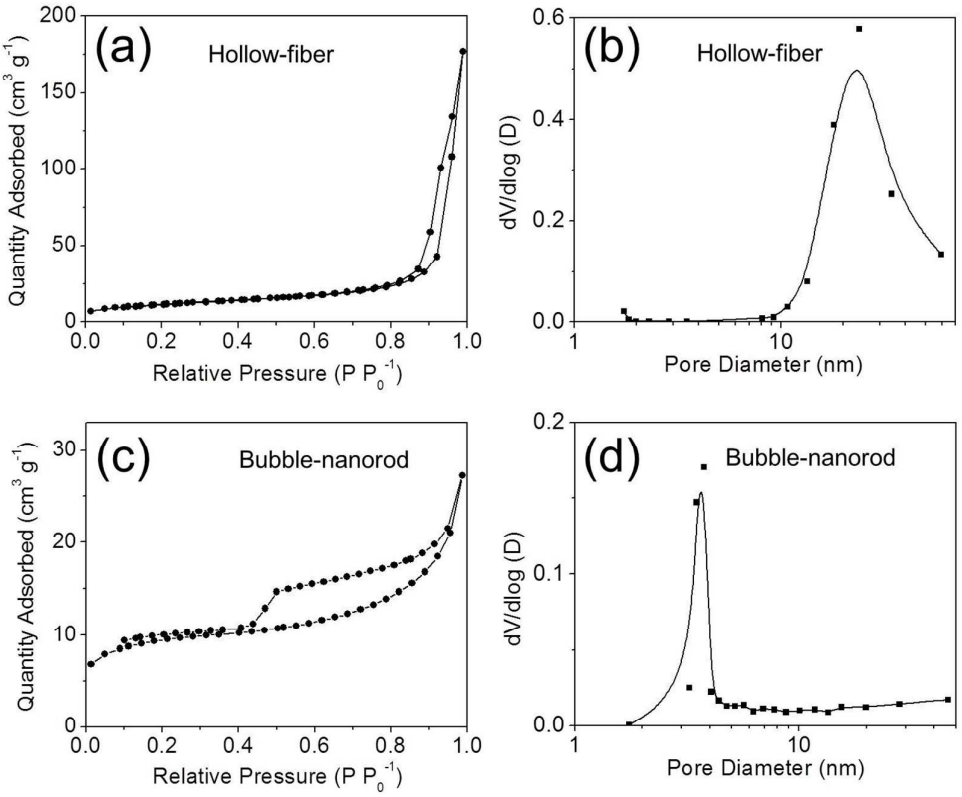

Figure S4. N_2 gas adsorption and desorption isotherms and pore size distributions: (a) and (b) hollow Fe_2O_3 nanofiber and (c) and (d) bubble-nanorod-structured Fe_2O_3-C nanofiber.

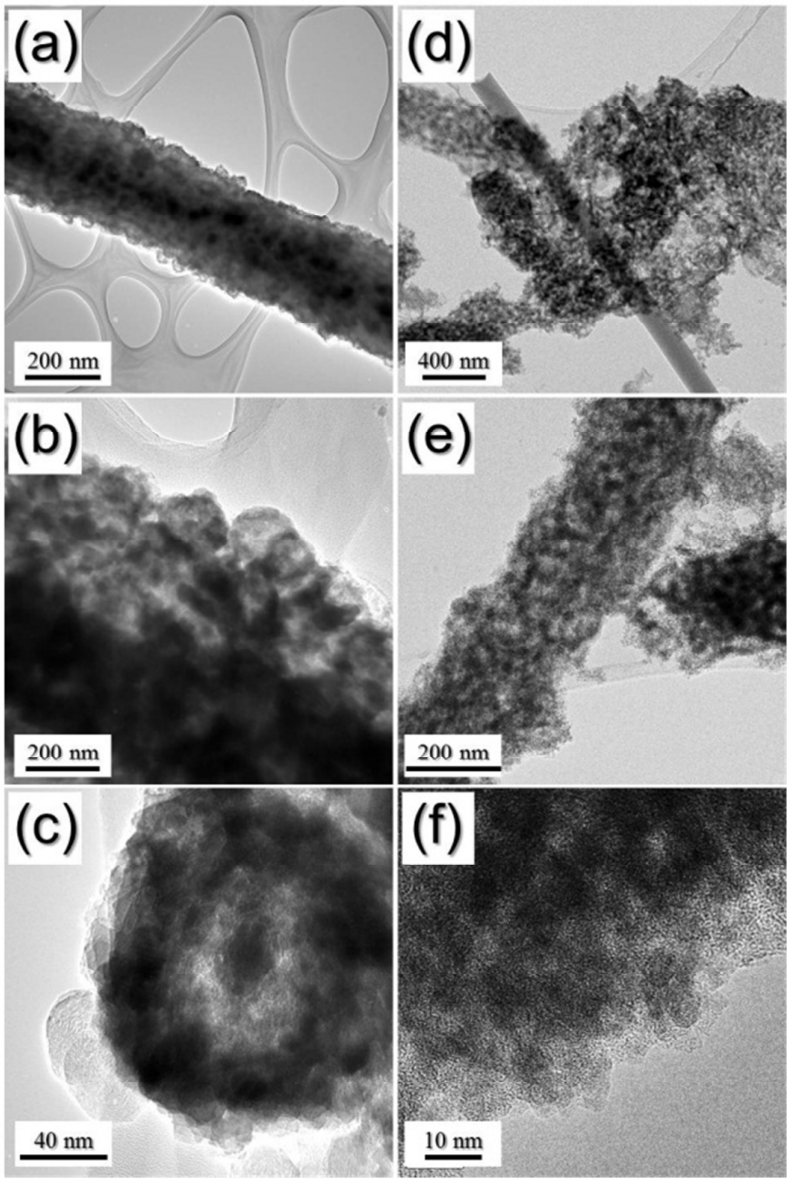

Figure S5. Morphologies of the (a)-(c) bubble–nanorod-structured Fe_2O_3–C composite nanofibers and (d)-(f) hollow bare Fe_2O_3 nanofibers obtained after 300 cycles.

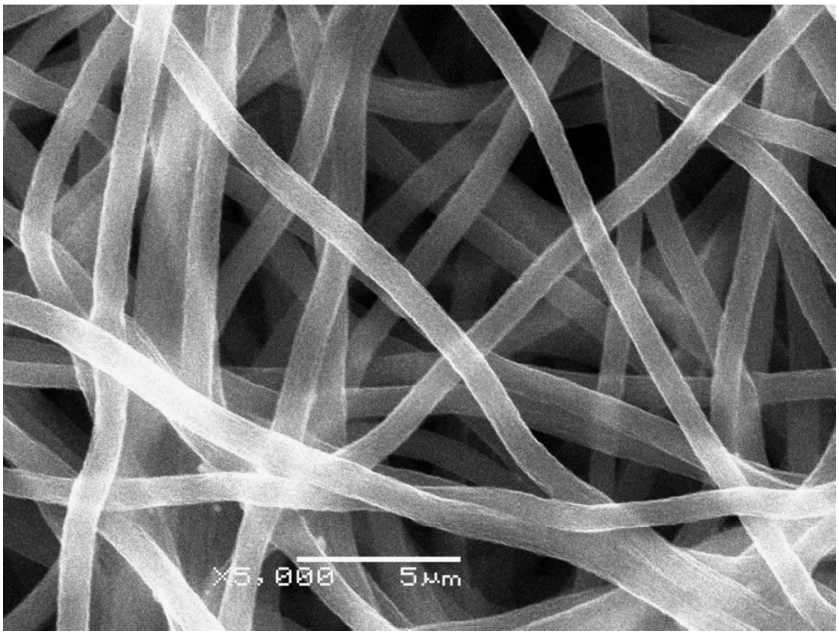

Figure S6. SEM image of electrospun nanofibers.

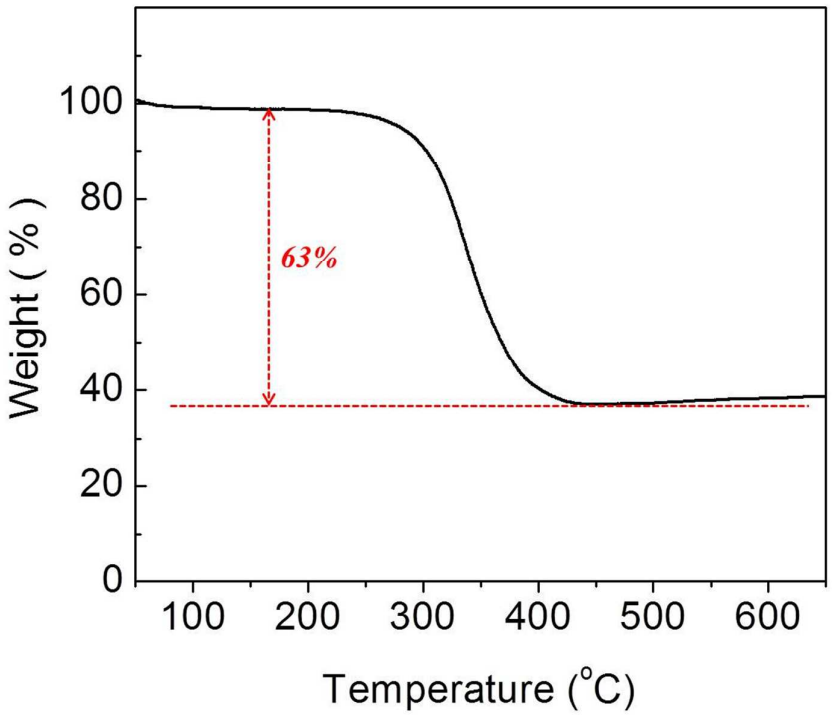

Figure S7. TG analysis of the nanofibers post-treated at 500 °C under H_2/Ar atmosphere.

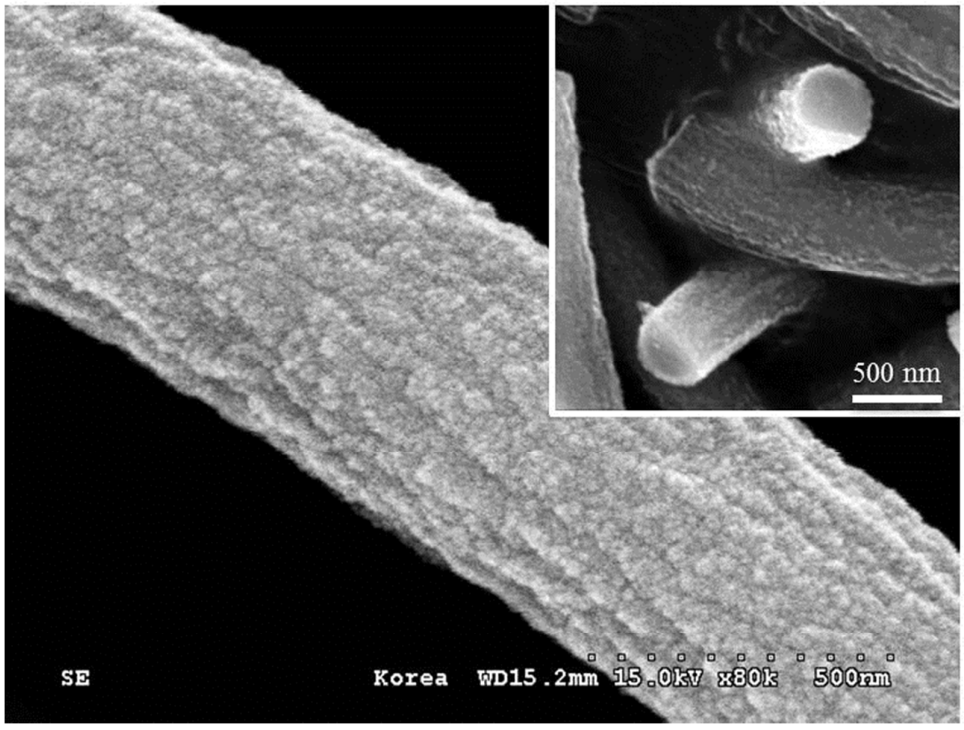

Figure S8. FE-SEM image of the bubble-nanorod-structured Fe_2O_3–C composite nanofiber and cross-section image of the nanofibers (inset image).

The formation mechanism of the hollow bare Fe_2O_3 nanofiber was confirmed by investigating the morphological changes of the electrospun nanofiber according to the post-treatment treatment temperatures under air atmosphere. Digital photos and SEM images of the nanofibers otained at different post-treatment temperatures are shown in **Figure S9**. The nanofibers obtained at a low post-treatment temperature of 300 ^oC had filled structure and black color. The electrospun nanofibers transformed into the FeO_x–C composite nanofibers at a low post-treatment temperature of 300 ^oC. However, the nanofibers obtained at post-treatment temperatures of 400 and 500 ^oC had fiber-in-tube and hollow structures, respectively. The color of the nanofibers obtained at post-treatment temperatures of 400 and 500 ^oC was red. The complete combustion of carbon material resulted in pure Fe_2O_3 nanofibers with red color at post-treatment temperatures of 400 and 500 ^oC. The FeO_x–C composite nanofiber was formed as an intermediate product during the early stage of the post-treatment process at temperatures of 400 and 500 ^oC. The complete combustion of FeO_x–C composite nanofiber under air atmosphere produced the fiber-in-tube Fe_2O_3 nanofiber. The combustion of the outer layer of the FeO_x–C composite nanofiber produced core-shell-structured FeO_x–C/Fe_2O_3 nanofiber. Combustion of the FeO_x–C composite did not occur inside the densely structured composite nanofiber because the supply of oxygen as the oxidant to the inside of the nanofiber was insufficient. The contraction of the inner FeO_x–C core part upon further heating produced the FeO_x–C@void@Fe_2O_3 fiber-in-tube nanofiber as an intermediate. The highly crystalline Fe_2O_3 shell formed by FeO_x–C combustion had low shrinkage. Finally, the combustion of the FeO_x–C inner fiber produced the Fe_2O_3@void@Fe_2O_3 fiber-in-tube nanofiber. In this study, the hollow bare Fe_2O_3 nanofiber at a high post-treatment temperature of 500 ^oC was formed by well-known Ostwald ripening mechanism during the heat-treatment process. The Ostwald ripening process transformed the Fe_2O_3@void@Fe_2O_3 fiber-in-tube nanofiber into the hollow bare Fe_2O_3 nanofiber. The Ostwald ripening process induces outward mass migration of small crystallites in the central part of nanofiber during the subsequent heat-treatment procedure, forming hollow structure of the resultant nanofiber.

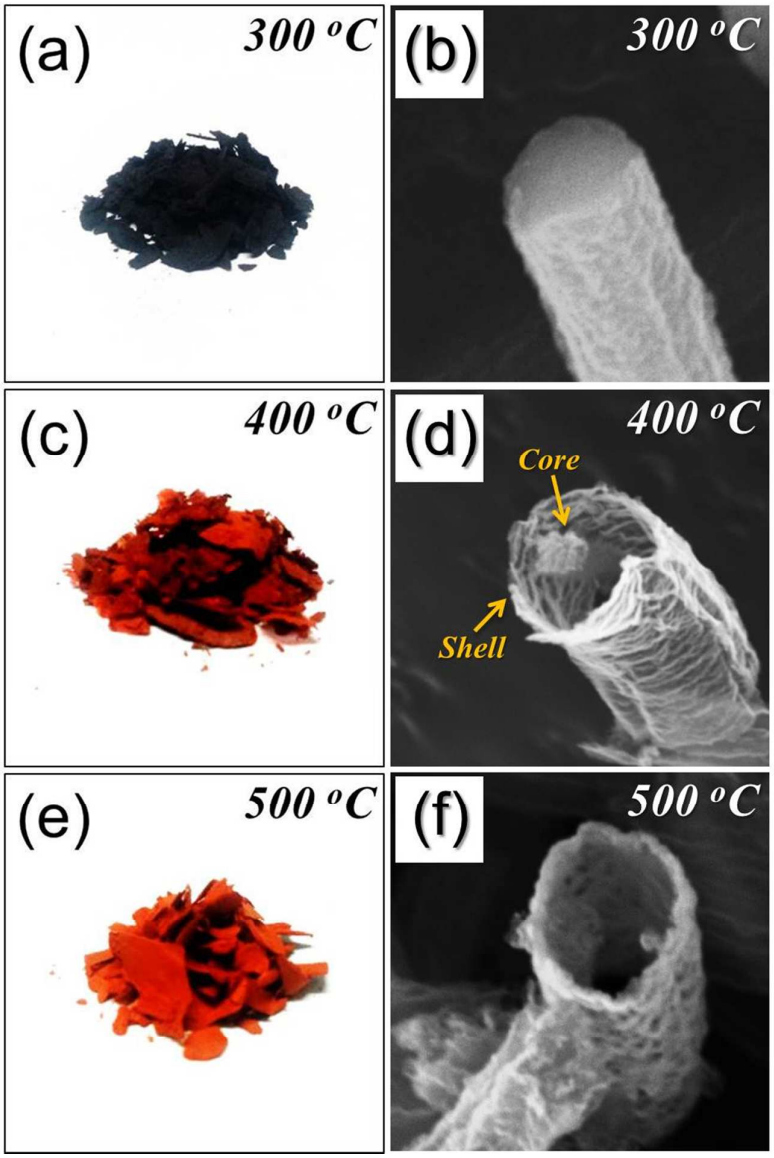

Figure S9. Digital photos and SEM images of the nanofibers obtained at different post-treatment temperatures under air: (a) and (b) 300 ^{o}C, (c) and (d) 400 ^{o}C, (e) and (f) 500 ^{o}C.

Figure S10 shows the electrochemical properties of the electrode with high concentration of active material. The anode was prepared by mixing the active material, carbon black, and sodium carboxymethyl cellulose (CMC) in a weight ratio of 8:1:1. The initial discharge and charge capacities of the bubble–nanorod-structured Fe_2O_3–C composite nanofibers at a current density of 1.0 A g^{-1} were 1365 and 937 mA h g^{-1}, respectively, and their corresponding initial Columbic efficiency was 69%. The discharge capacities of the bubble–nanorod-structured Fe_2O_3-C composite nanofibers for the 2nd and 300th cycles were 920 and 725 mA h g^{-1}, respectively.

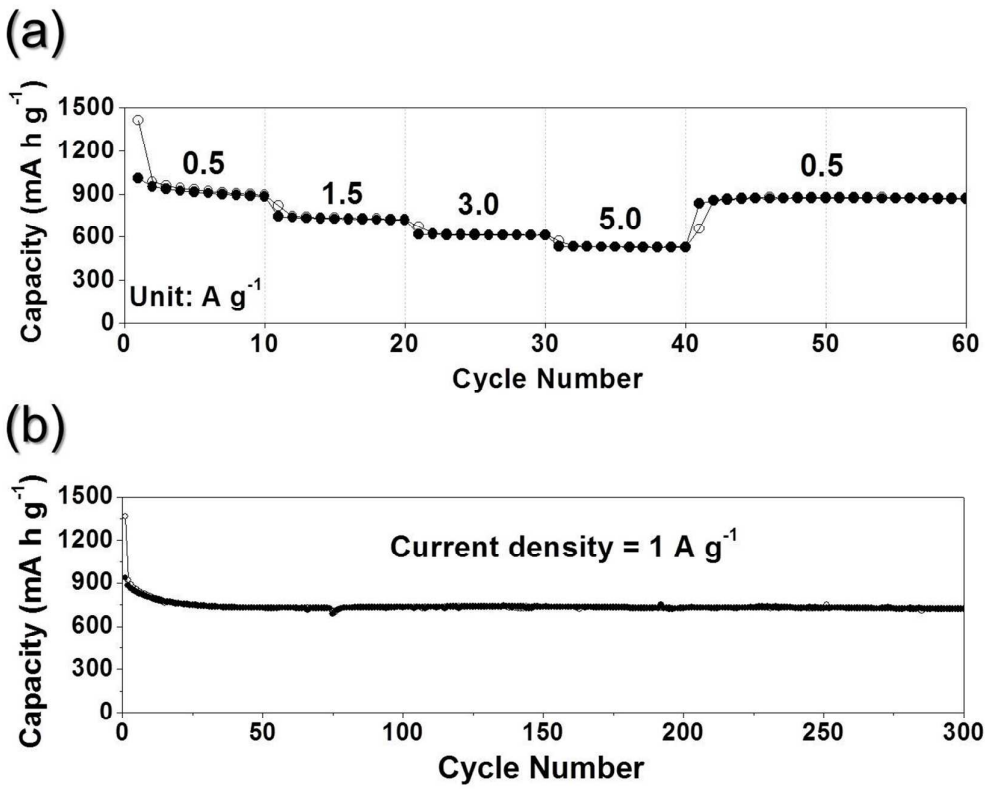

Figure S10. Electrochemical properties of the electrode with high concentration of active material: (a) cycling performance and (b) rate performance.

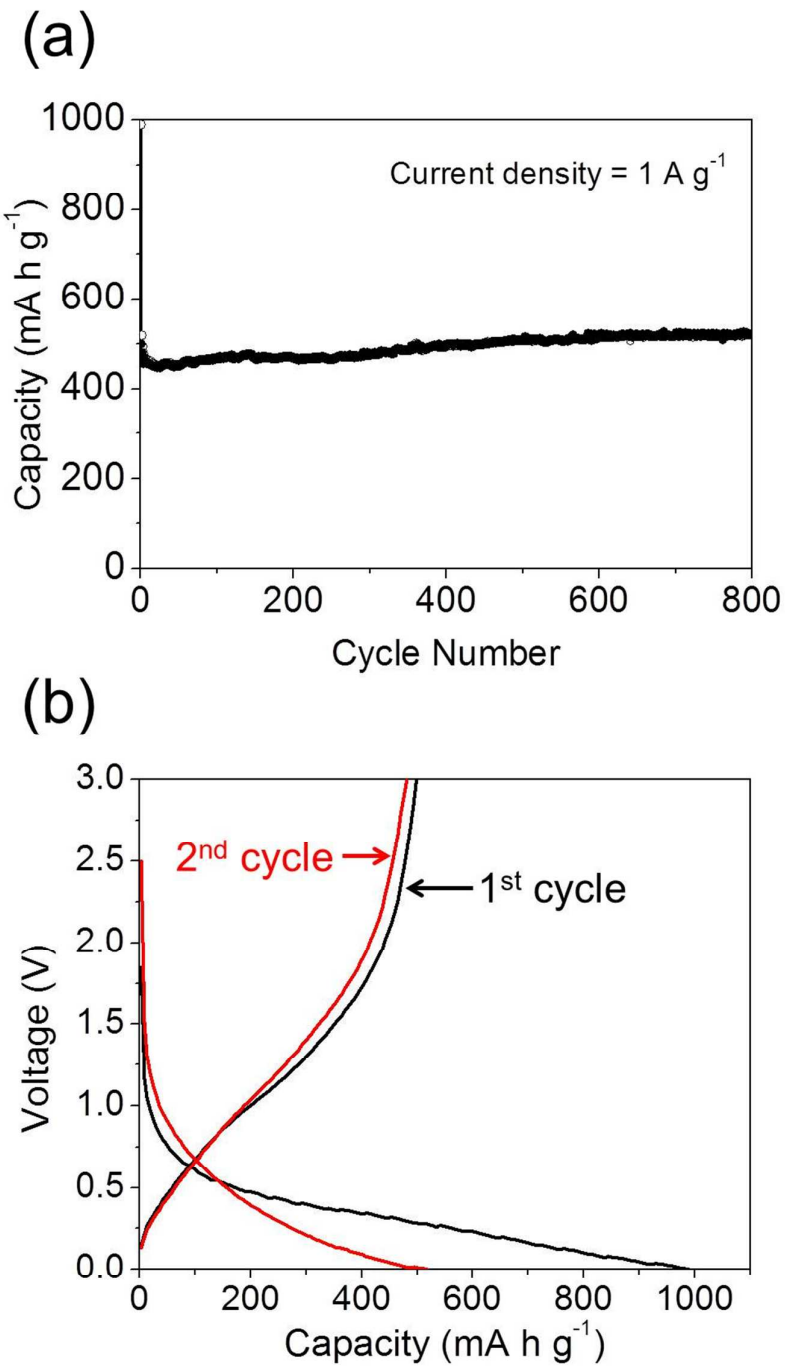

Figure S11. Electrochemical properties of FeO_x–carbon composite nanofibers after thermal-treatment at 500 ^{o}C under H_2/Ar gas atmosphere: (a) cycling performance and (b) charge-discharge curves.